

## Picosecond spectroscopy and hyperlinear photoluminescence in poly(para-phenylene)-type ladder polymers

G. Kranzelbinder

*Centro di Elettronica Quantistica e Strumentazione Elettronica-CNR, Dipartimento di Fisica, Politecnico Di Milano, piazza Leonardo da Vinci 32, I-20133, Milano, Italy*  
and *Institut für Festkörperphysik, Technische Universität Graz, Petersgasse 16, A-8010 Graz, Austria*

H. J. Byrne

*Physics Department, Dublin Institute of Technology, Kevin Street Dublin 8, Ireland*  
and *Max-Planck-Institut für Festkörperforschung, Heisenbergstrasse 1, D-70506 Stuttgart, Germany*

S. Hallstein and S. Roth

*Max-Planck-Institut für Festkörperforschung, Heisenbergstrasse 1, D-70506 Stuttgart, Germany*

G. Leising

*Institut für Festkörperphysik, Technische Universität Graz, Petersgasse 16, A-8010 Graz, Austria*

U. Scherf

*Max-Planck-Institut für Polymerforschung, Ackermannweg 10, D-55128 Mainz, Germany*

(Received 26 December 1996)

In our investigations of the photoluminescence in poly-(para-phenylene)-type ladder-polymer films a highly nonlinear dependence of the emission spectra is observable at elevated excitation densities. A spectral redistribution results in the hyperlinear increase of emission efficiency in the blue region, as the vibronic 0-1 transition ( $\lambda = 492$  nm) becomes the most predominant radiative relaxation. The detailed study of temporal decay and spectral evolution of luminescence provided by streak camera measurements performed in the temperature range  $T = 20$ – $300$  K reveals the spectrum being composed by the contributions of two different emitting species, namely,  $S_1$ -singlet states and aggregates. The material is found to be photochemically stable and luminescence does not seem to be limited by saturation effects even under high-excitation conditions, which is essential for laser application. [S0163-1829(97)03427-9]

### INTRODUCTION

The realization of highly efficient blue organic light-emitting diodes based on poly-paraphenylenes (PPP's) and polyphenylene oligomers has attracted much attention to these materials for their commercial potential to be utilized in optical technologies.<sup>1-3</sup> Together with the improvements in chemical synthesis, the intrinsic properties of these quasi-one-dimensional systems are less and less dominated by effects of the extrinsic nature and so a very vital theoretical discussion about the fundamental excitation processes and luminescence in different materials also has been stimulated.<sup>4,5</sup>

Different synthesis techniques of PPP,<sup>6,7</sup> bridging neighboring phenyl rings into a rigid sterically planar ladder-type structure, have succeeded in providing well-defined conjugated polymers of high structural regularity,<sup>8</sup> high quantum yield (90% in a solution and 30% in a solid state<sup>9</sup>), and high solubility due to large side groups (i.e., alkyl groups) attached to the backbone (Fig. 1). Moreover, a methyl-substituted poly-(para-phenylene)-type ladder polymer (m-LPPP) is a conjugated polymer in a solid state, in which stimulated emission is not in a competition with photoabsorption or other dissipative processes.<sup>10-12</sup> As will be shown in the following, this transition emitting in the blue-green

region does not saturate at the high intensities employed here; consequently, additional interest is applied to the utilization of m-LPPP in laser applications.

Since the sensitivity of the optical properties to the influence of oxygen has been demonstrated in previous experiments,<sup>8,13</sup> caution was taken by preparing the samples under Ar conditions. The polymer is dissolved in oxygen-free toluene (60 °C for 1 h) and films, dropcast onto infrasil substrates, are photochemically stable even under high illumination intensities. Photochemical stability is an essential property for technological application and therefore prompts

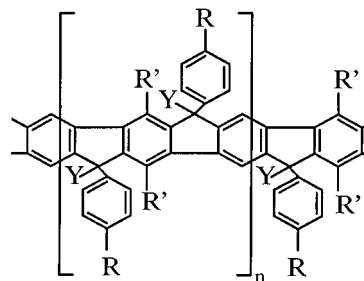


FIG. 1. Chemical structure of the PPP-type ladder polymer (m-LPPP).  $Y = \text{CH}_3$ ,  $R = \text{C}_{10}\text{H}_{21}$ ,  $R' = \text{C}_6\text{H}_{13}$ , and  $\hat{n} = 52$ .

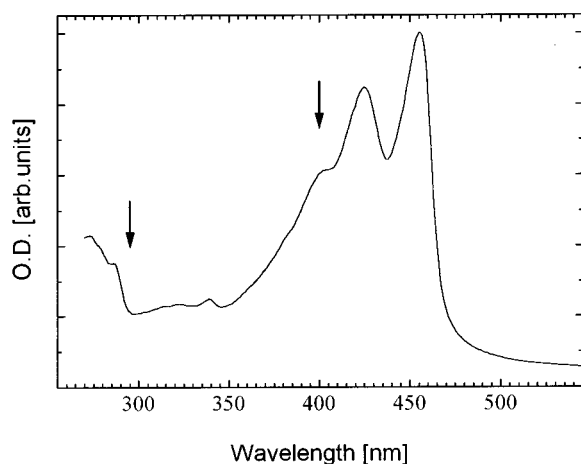


FIG. 2. Optical density (OD) of m-LPPP. The arrows indicate the excitation wavelengths used in the experiments.

the inviting idea to build a homopolymer solid-state laser based on this very material.

The absorption edge of this material (Fig. 2) possesses an onset that is very steep compared to poly-(*p*-phenylene vinylene) (PPV) or PPP.<sup>14</sup> Low subgap absorption<sup>15</sup> and the resolution of the vibronic transitions in the photoabsorption spectrum as well as the dominance of the zero-phonon peak indicates the high intrachain order and the narrow distribution of conjugation lengths in m-LPPP.<sup>8</sup> The photoluminescence recorded under steady-state conditions is characterized by two emission peaks ( $\lambda = 463$  and  $492$  nm) and a spectral broad component at lower energies ( $\lambda = 506$ – $630$  nm). Time-resolved measurements and the study of luminescence as a function of excitation intensity are the tools used in our investigations to differentiate between the components of the steady-state spectrum.

### EXPERIMENT

The high-intensity measurements were performed using a hybrid mode-locked dye-laser output amplified by six orders of magnitude in a pulse tuning amplifier (PTA) (Continuum 60) being pumped by a regenerative amplifier (Continuum 60-30) providing pulses specified with a full width at half maximum of 4 ps and energies of 1 mJ/pulse ( $\lambda = 590$  nm, with a repetition rate of 30 Hz). The PTA laser output was frequency doubled ( $\lambda = 295$  nm) and the high-intensity pulses were directed to the sample for excitation. The sample was investigated at room temperature ( $T = 300$  K) and under dynamic vacuum conditions ( $p = 10^{-5}$  mbar). The luminescence signal was detected by a diode array (DDA 1024) via a spectrometer (Cromex 250 mm) and data were processed by an optical simultaneous multichannel analyzer (Spectroscopy Instruments).

For the time-resolved measurements the sample, mounted in a He cryostat, was excited with frequency-doubled pulses ( $\lambda = 400$  nm) generated in a Ti:sapphire laser setup (Tsunami) and the luminescence was detected by a streak camera (Hamamatsu/Synchroscan) in combination with a spectrometer. The signal was recorded by a videocamera via a silicon intensified target and data processed. With this setup studies of the temporal decay and the spectral evolution of the pho-

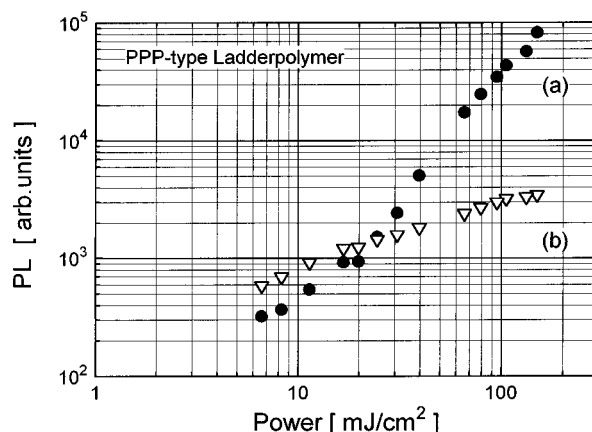


FIG. 3. Time-integrated luminescence in PPP ladder polymer vs excitation intensity: (a) hyperlinear response of the 0-1 transition and (b) sublinear behavior of the low-energy emission ( $\lambda = 506$ – $628$  nm integrated) at  $T = 300$  K.

toluminescence were performed as a function of temperature (20–300 K), achieving a total system resolution better than 10 ps.

### RESULTS AND DISCUSSION

The radiative relaxation of photoexcited species results in the photoluminescence (PL) spectrum. In this paper the luminescence is found to originate from two different emitting species, a conclusion that is supported by our studies of the decay dynamics and the behavior of luminescence as a function of excitation intensities (Fig. 3). In the short-wavelength region ( $\lambda < 520$  nm) the vibrational splitting seen in absorption is mirrored by the peaks of the 0-0 and 0-1 interband transitions, whereas at lower energies in the PL steady-state spectrum a broad component is most prominent in the solid state. Measurements in solid solutions at different concentrations<sup>9</sup> strongly indicate the intermolecular origin of the latter process, which we assign to the radiative decay of excited aggregates,<sup>14</sup> which are also seen in the unsubstituted form of the ladder-type polymer.<sup>16</sup>

The intrinsic nature of the high-energy interband luminescence is evidenced by the sharply pronounced features, representing radiative relaxation of the lowest vibrational singlet state to the vibrational manifold of the ground state. Steady-state measurements clearly show the 0-0 and 0-1 transitions, respectively, whereas due to the superposition with the spectrally broad component the 0-2 peak is observed only in the time-resolved streak camera measurement (Fig. 6).

Photoluminescence was investigated under high-excitation densities focusing picosecond pulses ( $\lambda = 295$  nm) with energies over the range 4–150 mJ/cm<sup>2</sup> on the m-LPPP film. In the transmission geometry employed here the spectral overlap between absorption and luminescence leads to a total self-absorption of the 0-0 contribution. On increasing the input intensities a highly nonlinear evolution of the photoluminescence characteristics is observed. In contrast to low-intensity excitation, the broad component is not the dominant emission feature since the optical process of the 0-1 transition undergoes a dramatic increase in luminescence efficiency, namely, over three orders of magnitude

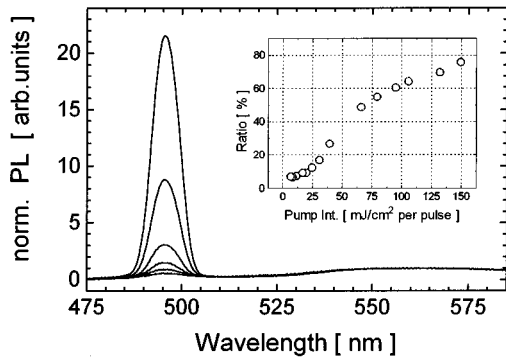


FIG. 4. Photoluminescence (spectra normalized to the emission peak at 560 nm) and pump intensities (curves from bottom to top): 17, 25, 31, 39, 66, and 133 mJ/cm<sup>2</sup> per pulse. The contribution of the 0-1 transition relative to the integrated PL is shown in the inset.

following a hyperlinear second-order behavior [the numerical fit  $\mathcal{P} \sim I^x$ , where  $\mathcal{P}$  denotes the PL, gives  $x = 1.9(\pm 0.1)$ ]. The broad luminescence component at longer wavelengths exhibits a sublinear response at high excitations, which can be described by a square-root dependence [the numerical fit  $\mathcal{P} \sim I^x$  gives  $x = 0.52(\pm 0.02)$ ] (Fig. 3).

We want to emphasize that in the blue-green region the absence of saturation effects even under these extreme illumination conditions has been illustrated and the measurements were shown to be reversible demonstrating the high photostability. On the other hand, in excitation experiments performed by a Ti:sapphire-laser-based system, with corresponding intensities three orders of magnitude lower, the luminescence exhibits a linear dependence on illumination. Therefore, we conclude with the possible existence of a threshold intensity indicating a critical excited-state density associated with the change from linear to hyperlinear behavior.

Phenomena associated with many-body processes have been extensively investigated for classical semiconductors<sup>17,18</sup> and are also seen in organic material such as fullerenes,<sup>19</sup> but in contrast to latter investigations a spectral evolution, i.e., a redshift of emission, corresponding to exchange/correlation energies, is not observed. We want to point out that the integral signal of luminescence ( $\lambda = 485\text{--}628$  nm) shows a more or less linear dependence. This possibly indicates a scenario in which the excitation of the emitting states as a function of intensity and temperature is determined by interaction processes specifying the excitation energy distribution. This idea is also supported by the fact that the path, as to be shown in the following, of relaxation from singlets to low energetic states is indeed observed. However, at high excitation intensities the vibronic 0-1 transition becomes the most efficient radiative relaxation channel, thus resulting in the dramatic increase of the PL signal at  $\lambda = 492$  nm (see Fig. 4). This is planned to be discussed in terms of cooperative radiation like optical superradiance and stimulated processes in a forthcoming paper.<sup>20</sup>

Further insight into the luminescence mechanism is attained by time-resolved measurements studying temporal decay and spectral evolution as a function of temperature. The luminescence spectrum is divided into three regions: the

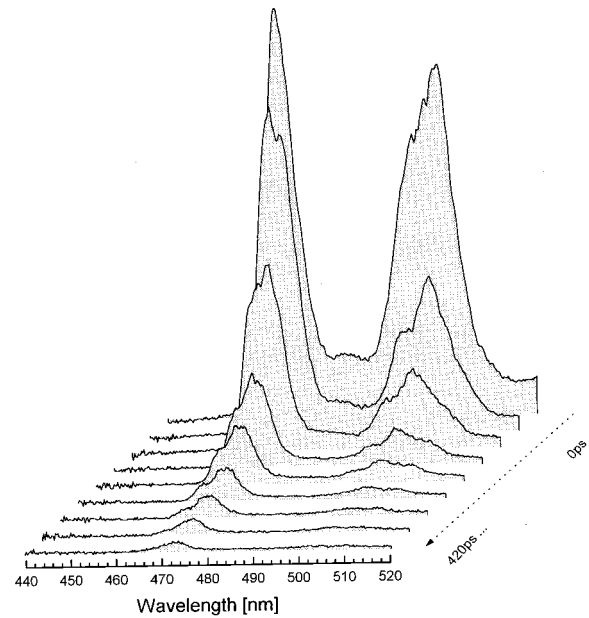


FIG. 5. Time-resolved photoluminescence at  $T=20$  K,  $\lambda_{\text{exc}}=400$  nm, and a time window 0–420 ps.

high-energy contribution in the blue-green region assigned to the 0-0 and 0-1 interband transitions (Fig. 5), a broad component in the yellow region, and a spectral region between 510 and 560 nm where the vibronic 0-2 transition is overlapped by the latter contribution (Figs. 5 and 6). With decreasing temperature we see that the interband peaks shift to longer wavelengths: for the 0-0 transition, 463 nm ( $T = 300$  K) and 469 nm (20 K) and for the 0-1 transition, 492 nm ( $T = 300$  K) and 500 nm (20 K). Whereas the total luminescence of the vibronic transitions of the interband emission is more or less constant in the range 300–150 K, a further reduction of temperature significantly enhances the quantum yield, which is increased by a factor of 4.5 (for the 0-0 transition) and 2.2 (for the 0-1 transition) at  $T = 20$  K. The time-resc

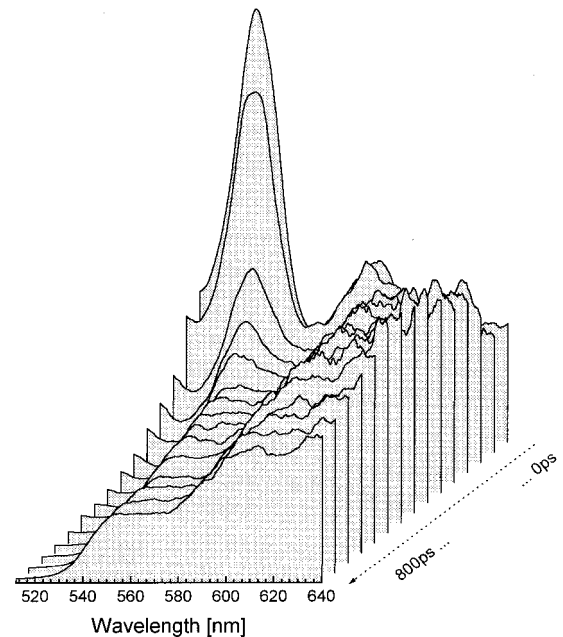


FIG. 6. Time-resolved photoluminescence at  $T=20$  K,  $\lambda_{\text{exc}}=400$  nm, and a time window 0–800 ps.

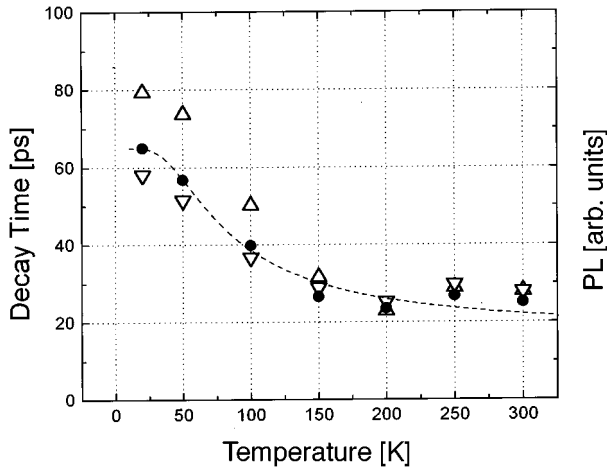


FIG. 7. Interband emission: decay times (single exponential fits) and quantum yield as a function of temperature for the 0-0 transition (up triangles), the 0-1 transition (down triangles), the quantum yield (solid circles), and the numerical fit (dashed line).

transitions (0-0, 0-1, and 0-2) undergoes a redshift of a typical 5 nm within the first 50 ps of temporal decay.

Various spectral cross sections of the streak camera measurements have been analyzed and evaluated numerically, providing an extensive study of the luminescence dynamics at different temperatures and wavelengths. Proper modeling of the signal decay can be quite delicate, especially when experimental data are not to be mimicked by a simple analytical function. In order to ensure physical significance in the fit parameters, we restricted the numerical analysis to single and double exponentials and evaluate values of 855 and 1055 ps for the aggregate emission at  $T=300$  and 20 K, respectively. The results of the exponential fits of the time constants of the vibronic 0-0 and 0-1 transitions as a function of temperature are summarized in Fig. 7. Whereas at room temperature a value of 28 ps is obtained using a single exponential, different spectral contributions of a long-lived background become more effective in the range below  $T=150$  K and therefore have been taken into account by a double exponential decay function.

As shown in Fig. 7, the decay times correspond to the quantum yield of the interband luminescence as a function of temperature. Contrarily, the time-integrated luminescence signal in the range 580–647 nm, not shown here, increases with temperature. This behavior indicates a transfer mechanism of excitation between the two states of emitting species and suggests the presence of a potential barrier separating those states. The potential barrier can be surmounted by thermal activation or by quantum mechanic tunneling providing a relaxation process of singlet states to lower-energy states, a picture that is also supported by the indication of formation time on the order of 100 ps detected at  $\lambda > 610$  nm in the low-temperature measurement ( $T=20$  K) (see Fig. 6). The spectral restriction of such an observation is possibly caused by the spectral overlap of the feature at  $\lambda=580$  nm that is to be attributed to a further vibronic satellite, also exhibiting a typical 60-ps decay at  $T=20$  K, which would therefore compensate for the signal onset associated with the effect of formation behavior in that region.

Assuming that the nonradiative transition to radiative

states located at lower energies is the only temperature-dependent one, the mechanism of energy transfer resulting in a reduced singlet emission  $I_{S1}$  can be expressed in the form

$$I_{S1}(T)^{-1} = I_{S1}(T=0 \text{ K})^{-1} + A \exp(E_B/kT),$$

a concept that has already been invoked to explain intramolecular self-trapping processes caused by strong exciton-lattice interaction in pyrene<sup>20</sup> and PPV.<sup>21–23</sup> From this equation the potential height  $E_B$  may be calculated to 13 ( $\pm 3$ ) meV. Furthermore,  $E_B$  was evaluated independently by fitting the corresponding luminescence increase in the yellow region giving a value of 16.5 ( $\pm 3.0$ ) meV. Therefore, the potential barrier separating singlet exciton states and those of aggregate emission can be estimated to 15 ( $\pm 3$ ) meV. The fact that femtosecond pump and probe experiments at room temperature<sup>10</sup> do not indicate such formation effects<sup>10</sup> coincides with this result since, like we see in our streak camera measurements ( $T=20$ –300 K), with  $E_B$  just on the order of magnitude of  $kT$ , the influence of this barrier is to be detected only in a low-temperature experiment.

## SUMMARY

In order to elucidate the mechanism of excitation relaxation in m-LPPP films the spectral evolution and the temporal decay of luminescence was investigated by streak camera measurements providing further insight in the relaxation dynamics. The PL spectrum is composed of the contribution of two radiative species. The vibronic transitions of singlet states constitute the spectrally sharp components in the blue-green region (peaks at  $L=463$ , 492, and 536 nm), which are intramolecular in origin. These luminescence contributions decay with typical time constants evaluated to 28 ps ( $T=300$  K) and 60 ps ( $T=20$  K). On the other hand, a spectrally broad and long-lived component with decay times of 855 ps ( $T=300$  K) and 1055 ps ( $T=20$  K) is attributed to aggregate emission observed at longer wavelengths.

Luminescence yields studied in different spectral regions as a function of temperature ( $T=20$ –300 K) indicate the presence of a potential barrier  $E_B$ , 15 meV in magnitude. It is shown that singlet excitons surmounting this barrier by thermal activation or quantum-mechanical tunneling can relax to the aggregate states emitting at lower energies.

At high excitation conditions the latter component follows increasing intensities in a sublinear way, whereas quantum efficiency in the blue region is dramatically enhanced as the vibronic 0-1 interband transition ( $\lambda=492$  nm) becomes most efficient and increases in a second-order hyperlinear behavior. High photostability and the absence of saturation effects even under elevated excitation conditions together with stimulated emission in the blue-green region make m-LPPP a material to be applied as the active medium in a homopolymer-based solid-state laser.

## ACKNOWLEDGMENTS

The financial support from the Max-Planck-Institut für Festkörperforschung and from the SFB Elektroaktive Stoffe is gratefully acknowledged.

- <sup>1</sup>G. Grem, G. Leditzky, B. Ullrich, and G. Leising, *Adv. Mater.* **4**, 36 (1992).
- <sup>2</sup>S. Tasch, A. Niko, G. Leising, and U. Scherf, *Appl. Phys. Lett.* **68**, 1090 (1996).
- <sup>3</sup>F. Meghdadi, G. Leising, W. Fischer, and F. Stelzer, *Synth. Met.* **76**, 113 (1996).
- <sup>4</sup>K. Pakbaz, C. H. Lee, A. J. Heeger, T. W. Hagler, and D. McBranch, *Synth. Met.* **64**, 295 (1994).
- <sup>5</sup>H. Bässler, M. Gailberger, R. F. Mahrt, J. M. Oberski, and G. Weiser, *Synth. Met.* **49–50**, 341 (1992).
- <sup>6</sup>U. Scherf and K. Müllen, *Makromol. Chem. Rapid Commun.* **12**, 498 (1991).
- <sup>7</sup>U. Fahrenstich, K. H. Koch, M. Pollmann, U. Scherf, M. Wagner, S. Wegener, and K. Müllen, *Makromol. Chem.* **54/55**, 465 (1992).
- <sup>8</sup>W. Graupner, S. Eder, M. Mauri, G. Leising, and U. Scherf, *Synth. Met.* **69**, 419 (1995).
- <sup>9</sup>J. Stampfl, S. Tasch, G. Leising, and U. Scherf, *Synth. Met.* **71**, 2125 (1995).
- <sup>10</sup>W. Graupner, G. Leising, G. Lanzani, M. Nisoli, S. De Silvestri, and U. Scherf, *Phys. Rev. Lett.* **76**, 847 (1996).
- <sup>11</sup>W. Graupner, G. Leising, G. Lanzani, M. Nisoli, S. De Silvestri, and U. Scherf, *Chem. Phys. Lett.* **246**, 95 (1995).
- <sup>12</sup>M. Yan, L. J. Rothberg, F. Papdimitrakopoulos, M. E. Galvin, and T. M. Miller, *Phys. Rev. Lett.* **72**, 1104 (1994).
- <sup>13</sup>W. Graupner, M. Mauri, J. Stampfl, and G. Leising, *Solid State Commun.* **91**, 7 (1994).
- <sup>14</sup>J. Stampfl, W. Graupner, G. Leising, and U. Scherf, *J. Lumin.* **63**, 117 (1995).
- <sup>15</sup>M. Moser and G. Leising, *Synth. Met.* **89**, 651 (1997).
- <sup>16</sup>U. Lemmer, S. Heun, R. F. Mahrt, U. Scherf, M. Hopmeier, U. Siegner, E. O. Göbel, K. Müllen, and H. Bässler, *Chem. Phys. Lett.* **240**, 373 (1995).
- <sup>17</sup>*Physics of Highly Excited States*, edited by M. Ueta and Y. Nishina, *Lecture Notes in Physics* Vol. 57 (Springer, Berlin, in press).
- <sup>18</sup>*Electron-Hole Droplets in Semiconductors*, edited by C. D. Jeffries and L. V. Keldish (Springer-Verlag, Heidelberg, 1976).
- <sup>19</sup>H. J. Byrne, L. Akselrod, A. T. Werner, W. K. Maser, M. Kaiser, W. W. Rühle, and S. Roth, in *Science and Technology of Fullerene Materials*, edited by P. Bernier, D. S. Bethune, L. Y. Chiang, T. W. Ebbesen, R. M. Metzger, and J. W. Mintmire, *MRS Symposia Proceedings* No. 359 (Materials Research Society, Pittsburgh, 1995), p. 451.
- <sup>20</sup>G. Kranzelbinder, G. Lanzani, M. Nisoli, W. Graupner, S. De Silvestri, G. Leising, and U. Scherf (unpublished).
- <sup>21</sup>A. Matsui, K. Mizoni, N. Tamai, and I. Yamazaki, *Chem. Phys.* **113**, 111 (1987).
- <sup>22</sup>M. Furukawa, K. Mizuno, A. Matsui, S. D. D. V. Ruughooputh, and W. C. Walker, *Jpn. Soc.* **58**, 2976 (1989).
- <sup>23</sup>T. Kobayashi, *Relaxation in Polymers* (World Scientific, Singapore, 1993), p. 6.